Original article

Textile Research Journal

Textile Research Journal
82(5) 443–453

DOI: 10.1177/0040517511427969
trj.sagepub.com

SAGE

3D geometrical modelling of tubular braids

Tuba Alpyildiz

Abstract

Geometrical modelling for tubular braids of different structures is studied and a simple versatile three-dimensional model is proposed after considering the crimp of the braiding yarn together with the tubular curvature of the tubular braid structure. The proposed model is versatile and suitable not only for different braid structures, but also, with the changes in the structural parameters such as braid angle, number of yarns in a set, yarn and mandrel diameter the model is still applicable. Application and 3D drawings of the model for diamond, regular and triaxial braids are given with the aid of Visual Basic and 3DSMax Studio.

Keywords

Geometrical model, braid, diamond braid, regular braid, triaxial braid

Introduction

Braiding is the intertwining of yarns at a defined angle (braid angle) between the longitudinal axes of the structure and the yarns in a desired braid structure. Most common braid structures are diamond (1/1) braid, where each yarn crosses above and below the other yarn in a repeating manner, and regular (2/2) braid, where every yarn crosses above two and below two other yarns of the set moving in the opposite direction in a repeating manner. It is also possible to add axial yarns in the longitudinal direction and to obtain triaxial braids. Braids with the mentioned structures can be flat or tubular.

Tubular braiding has traditionally been used for the manufacture of textile structures such as ropes, but in recent years braiding is increasingly being used in aviation, medical applications, sporting goods, mechanical and civil engineering applications whether as itself or as reinforcement within composites. Among the composite applications it competes with filament winding, pultrusion and tape lay-up methods. Even by using mandrels of different cross-sectional shapes, 3D braided preforms can be obtained.

In order to perform engineering analysis of the structures, it is important to develop theoretical models. These models build the relationship between the machine parameters and the geometry of the braids to be used in the prediction of the mechanical behaviour. Geometrical modelling is for the definition of the unit cell and is needed to predict the mechanical behaviour of braids. In addition to being the starting point for the analysis of failure mechanisms, the geometry of the braid structure, whether to be used alone or as a reinforcement in the composite, is also the starting point for the manufacture of the braids because geometrical models are useful to simulate the braided structure before manufacturing. In this way, it can be possible to optimize the braid structure for desired performance criteria.

The studies on the geometrical definition of the tubular braided structures started with Brunnschweiler,[1] as he derived 2D structural parameters of small diameter braids made of staple fibres to simulate the length of the braid using mathematical formulations. These were based on Pierce's assumptions of woven fabrics, and were to be used in the calculations of the extensions at break. Goff[2] introduced a crimp effect into the

Dokuz Eylul University, Turkey.

Corresponding author:
Tuba Alpyildiz, Dokuz Eylul University, Textile Engineering Department, Tinaztepe Campus, Buca, 35160 Izmir, Turkey
Email: tuba.alpyildiz@deu.edu.tr

geometric calculations of the braids by using numerical integration to obtain the path of a braiding yarn.

Among the studies on tubular braids, Phoenix[3] studied the tubular diamond braid with an elastic core and calculated the yarn length as a complete integral of a second kind. Wu et al.[4] focused on deriving a physical model for tubular small double braided ropes, subjected to either simple tension or simultaneous action of tension and bending, by defining a position vector for the braiding strand. Carey et al.[5] considered a sinusoidal trajectory to give a 2D configuration for only the undulation of the braiding yarns while proposing a model to predict the longitudinal elastic modulus of tubular braided composites. Mechanical responses of hybrid tubular braids were investigated by Hristov et al.[6] based on the braid geometry defined by numbers of tangential vectors. Hopper et al.[7] also studied on the mechanics of a hybrid tubular braid with an elastic core but the yarn crimp was excluded in the calculations of the geometrical parameters. Yüksekkaya and Adanur[8] investigated the tubular braided structures intended for medical applications; the relationship between the braid angle, helical length, braid diameter and elastic radial force were developed but the yarn crimp was ignored. Ayranci and Carey[9] have summarized the studies on the models for predicting the elastic constant of 2D braided composites and it was indicated that very few of the models used to predict the tubular braiding structure's elastic constants, consider the tube curvature in the geometric definition of the unit cell until improvements were introduced on certain existing models to compensate for the curvature in the unit cell. Later Endruweit and Long[10] proposed a model for the in-plane permeability of triaxially tubular braids, but for the characterization of the braid properties, the tubes were considered to be sliced and unrolled to flat sheets.

In these studies[1–10] on tubular braids, geometrical definitions such as yarn length are given, but such parameters are defined two-dimensionally to be considered in physical modelling, so the yarn paths are not defined which is needed for simulation of the braid structure. Only the necessary geometric parameters were derived[1–8] to be used in predicting certain performance behaviours, or position vectors were used in defining the braid structure,[3,5] or the yarn crimp was not included[7,8] in the calculations, or the tube curvature was not considered.[9,10]

When studies on triaxial braids are examined, among them Byun[11] has proposed a model to predict the elastic constants of the triaxially flat braided composite based upon the unit cell geometry of the reinforcement and thus, as a start, geometrical calculations for the triaxial flat braid were carried out with the assumption that the undulation was to be in the form of an arc. Ivanov et al.[12] focused on geometrical features, mechanical properties and damage initiation in a triaxially flat braided composite. As a start the characterization of the 3D architecture of the reinforcement which was a triaxial flat braid has been defined through geometrical considerations. Zhang et al.[13] proposed an analytical model for predicting the elastic properties of triaxially flat braided composite based on the iso-strain and interfacial continuity conditions. In terms of geometric definitions of the reinforcement the braider yarn cross-sections and the yarn length were defined. Xiao et al.[14] also studied a proposal for a model to predict the elastic constants of the triaxial flat braided composite, but in order to be able to predict the strength of the composite a geometric definition of the structure's unit cell was proposed where the yarn crimp was represented by a set of simple straight lines. So the studies[10–14] on triaxial braids are mainly focused on the flat braids.

None of the above given studies propose three-dimensional yarn paths which are needed for the simulation of the braid geometry, but there are also a few studies on the braids where the yarn paths are defined in three-dimensions. Lomov et al.[15] studied flat braids and proposed a geometrical model by giving the paths of the yarn centrelines within a predetermined unit cell. Liao and Adanur[16] aimed to develop 3D yarn shapes for tubular braids by the Frenet frame approach which meant developing each yarn by sweeping a closed curve along a centreline path where the closed curves and the centreline path represent the cross-sectional shape and the centreline configurations of the constituent yarns. The model was applied for diamond and regular braids by using coordinate frame techniques for sweeping the yarn with a 2D contour and a 3D trajectory as its centreline. Complicated expressions were used for trajectories that were not arc-length parameterized. Thus it was indicated that the solutions of the resulting equations could give rise to numerical difficulties and a general class of possible trajectories was needed to be obtained. The visualization was performed by OpenGL graphics system. However, this model does not consider the braid structure and the structural parameters so it is not applicable with different braid structures and the changes in the structural parameters can not be implemented into the model. Potluri et al.[17] introduced a computer controlled braiding machine to manufacture triaxial tubular braids and the braided structure has been simulated using virtual reality modelling language by sweeping the 2D cross-sectional area along a 3D path, however, the crimp/undulation of the braiding yarns has been ignored. Rawal et al.[18] studied tubular braids and presented 3D coordinates of the braiding yarn paths over different mandrels with different cross-sections, but they have ignored the yarn crimp (the sinusoidal path in the radial direction).

An accurate geometric modelling of braids is essential for accurately defining and predicting the mechanical properties of the structure. So realistic geometric modelling is fundamental as it is the starting point in modelling the deformability of structures. It is also important for a geometrical model to be put simply but not less realistic. In this study, a simple 3D geometrical model for the yarn paths composing tubular braids, which takes into consideration the crimp of the braiding yarn and is versatile to be used for braids with different structural parameters, has been given. The model proposed has been applied for diamond and regular tubular braids, and also for the triaxial diamond tubular braid. 3D simulation and presentation of the model applications have also been given.

Creation of the model

Assumptions

In the model, the yarns are assumed to be non-compressible and yarn cross-sections are assumed to be elliptical within the structure. A flattening coefficient is given, as below, so that the minor diameter (denoted by a) and major diameter (denoted by b) of the yarn cross-section within the braid structure can be calculated in terms of the yarn diameter, as yarn is on the bobbin.

$$e = a/b,\ e < 1 \tag{1}$$

$$\frac{\pi d^2}{4} = \frac{\pi ab}{4} \tag{2}$$

where e is the flattening coefficient, a and b are the minor and major diameter of the yarn within the braid, d is the yarn diameter prior to braiding.

Braiding yarns in the aimed structures are considered to have the same minor and major diameters and the cross-section of the yarns is uniform through the yarn length within the braid structure.

The crimp of the braiding yarns are assumed to be sinusoidal and along the braid length the yarn sets are assumed to follow a helical path with radius r_0 around a cylindrical mandrel which has a radius of R. So while the braiding yarn is following a sinusoidal curve it will be wound helically around a mandrel. As one set of yarns is revolving in the clockwise direction the other set will be revolving in the counter-clockwise direction.

There is no yarn slippage within the structure during and after the braiding process.

For the triaxial braid structure, the axial yarns which are placed in the longitudinal direction of the structure are assumed to be elliptical having the same minor and major diameters as the braiding yarns in the cross-section. They are also assumed to be uniform and straight. These straight yarns affect only the cross-over points where they are placed by shifting each braiding yarn at these crossover points with an amount of half of the minor diameter of the axial yarn cross-section.

Equation derivation

As the yarn sets for different types of braid structures follow a helical path, the equations giving the helical path along the mandrel will be the same for different types of the structures braided on a cylindrical mandrel. So the derivation of these equations is only given for the diamond braid structure as it is the basic structure. But for the sinusoidal path which the braiding yarn is to follow while helically wound onto the mandrel needs to be defined simply for different braid structures.

Equations for diamond braid structure

In the diamond braid, while one set of yarns are braided in the clockwise direction the other set will be braided in the counter-clockwise direction by each set crossing over and under the other set of yarns; one yarn over the other at each crossover point while at the next crossover point the placement of the yarns are vice versa.

The braiding yarns follow a helical path with a constant helix angle, which is the braid angle with the horizontal axes, over the cylindrical mandrel as shown in Figure 1.

The general equations giving such a helical yarn path are as:

$$X = r_0 \cos\theta \tag{3}$$

$$Y = r_0 \sin\theta \tag{4}$$

$$Z = r_0(\tan\alpha)\theta \tag{5}$$

Here α is the braid angle (constant helix angle with the horizontal axes), r_0 is the radius of the tubular braid and θ is the wrapping angle on the mandrel where $0<\theta<2\pi$ for one complete helix. For the braiding yarns revolving in the opposite direction on the same mandrel '$-\theta$' shall be taken. The radius of the mandrel can be defined as $R = r_0 - a$ where a is the minor diameter of the braiding yarn.

While one set of braiding yarns are helically wound onto the mandrel, they have a yarn crimp (undulation), due to the other set of braiding yarns moving in the

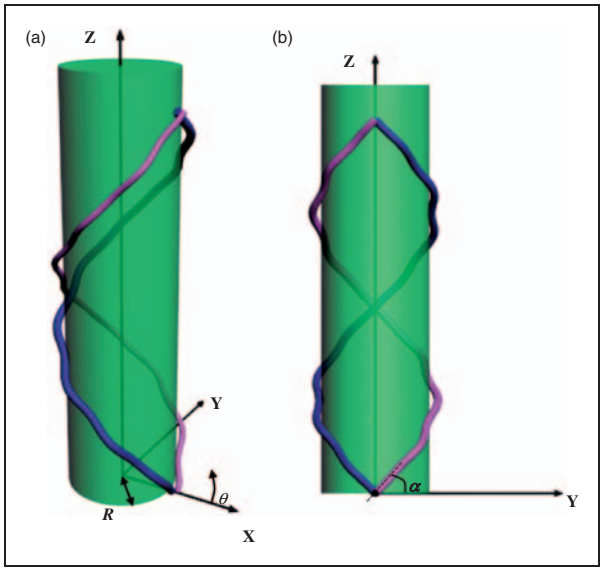

Figure 1. The path of the braiding yarns (one from the set of braiding yarns moving in the counter-clockwise direction and one from the set of braiding yarns moving in the clockwise direction) on the cylindrical mandrel (a) set of axes on perspective view, (b) side view.

opposite direction by crossing over/under, which is defined by a sine wave. To define this sine wave the braiding yarns are opened up on the ZX plane (Figure 2).

In Figure 2, 'n' and 'm' represent sets of braiding yarns moving in opposite directions, β is the shift angle between the braiding yarns moving in the same direction (Figure 3). On the mandrel the distance between the two braiding yarns moving in the same direction can be expressed by $r_0\beta$. And if the distance along the braiding yarn between the two crossover points is denoted by p then the below equations can be written where n is the number of braiding yarns moving in the same direction:

$$2\pi r_0 = n r_0 \beta \Rightarrow \beta = \frac{2\pi}{n} \tag{6}$$

$$p = \frac{r_0 \beta}{2\cos\alpha} \tag{7}$$

The yarn crimp of the braiding yarn is given in Figure 4 by considering $X^{\prime}$ to be the axes of the aforementioned sine wave of the braiding yarn and $Y^{\prime}$ to be the axes perpendicular to ZX plane and also to $X^{\prime}$.

In Figure 4, one of the braiding yarns revolving in the counter-clockwise direction is considered and the crossing over/under of the opposite braiding yarns

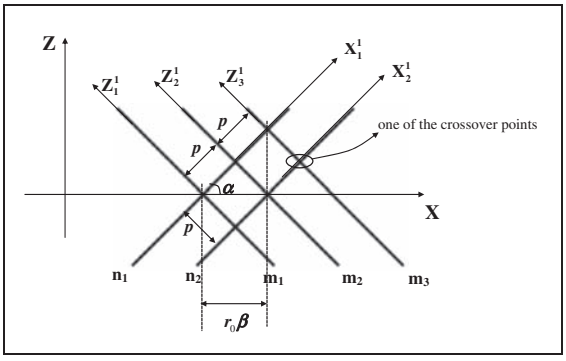

Figure 2. The helical path of the braiding yarns on ZX plane and $Z_i^1X_i^1$ axes system where Y_i^1 is perpendicular to $Z_i^1X_i^1$ plane.

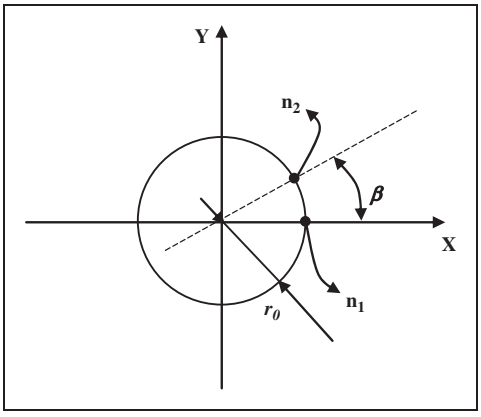

Figure 3. Shifting of the braiding yarns moving in the counter-clockwise direction (view on XY plane).

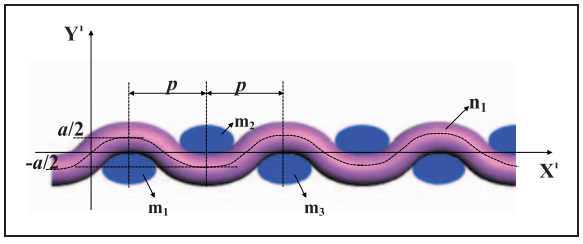

Figure 4. Crimp path of the braiding yarn revolving in the counter-clockwise direction for diamond braid structure (this axes system can be seen in relation with XYZ coordinate system in Figure 2).

expressed by m_1, m_2, m_3 can be seen. The crimp (undulation) path of this braiding yarn can be written as:

$$Y^1 = \frac{a}{2}\sin(kX^1) \tag{8}$$

where a is the minor diameter of the cross-section of the braiding yarn, $a/2$ is the amplitude and $2\pi/k$ defines the period which is equal to $2p$.

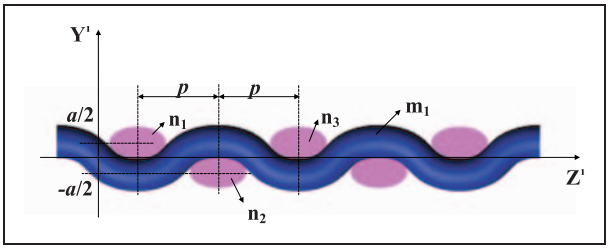

Figure 5. Crimp path of the braiding yarn revolving in the clockwise direction for diamond braid structure (this axes system can be seen in relation with XYZ coordinate system in Figure 2).

$$\frac{2\pi}{k} = 2p = \frac{r_0\beta}{\cos\alpha} \Rightarrow k = \frac{2\pi\cos\alpha}{r_0\beta} \tag{9}$$

Considering equation 9, X^t can be expressed in terms of the wrapping angle, θ, as $\frac{r_0\theta}{\cos\alpha}$ and when the crimp path of the braiding yarn (as a sine wave) is written on X^tY^t axes system in terms of the wrapping angle, θ, the following equation is obtained:

$$r(\theta) = \frac{a}{2}\sin\left(\frac{2\pi}{\beta}\theta\right) \tag{10}$$

When the general yarn path equations of the braiding yarns revolving in the counter-clockwise direction is written by superimposing the braiding yarn crimp and including the shifting angle the following equations are obtained:

$$r_0 = \frac{2p\cos\alpha}{\beta} \tag{11}$$

$$r(\theta) = \frac{a}{2}\sin\left(\frac{2\pi}{\beta}\theta + \frac{\pi}{2}\right) \tag{12}$$

$$X_i = (r_0 + r(\theta))\cos(\theta + (i-1)\beta), i = 1, 2 \ldots n \tag{13}$$

$$Y_i = (r_0 + r(\theta))\sin(\theta + (i-1)\beta), i = 1, 2 \ldots n \tag{14}$$

$$Z_i = r_0 \tan\alpha\theta, i = 1, 2 \ldots n \tag{15}$$

where p is the distance between the crossover points, a is the minor diameter of the yarn cross-section, r_0 is the radius of the tubular braid, $r(\theta)$ is the crimp of braiding yarn as a sine wave, β is the shift angle between the braiding yarns moving in the same direction, α is the braiding angle with the horizontal axes, n is the total number of the braiding yarns revolving in the same direction, i is the counter defining the actual braiding yarn revolving in the same direction and θ is the wrapping angle (variable) around the mandrel ($0<\theta<2\pi$).

For the braiding yarns moving in the clockwise direction, the same sine wave (with the same amplitude and period) will be used but at the crossover points, where the braiding yarns in the counter-clockwise direction are above the ones moving in the clockwise direction, they are below the crimp path in Y^tZ^t axes, as in Figure 5.

Thus the yarn path in terms of wrapping angle θ is as below:

$$r(\theta) = \frac{a}{2}\sin\left(\frac{2\pi}{\beta}\theta + \frac{\pi}{2} + \pi\right) \tag{16}$$

So the general yarn path equations of the braiding yarns revolving in the clockwise direction are written by superimposing the braiding yarn crimp and including the shifting angle as:

$$r_0 = \frac{2p\cos\alpha}{\beta} \tag{17}$$

$$r(\theta) = \frac{a}{2}\sin\left(\frac{2\pi}{\beta}\theta + \frac{3\pi}{2}\right) \tag{18}$$

$$X_i = (r_0 + r(\theta))\cos(-\theta - (i-1)\beta), i = 1, 2 \ldots n \tag{19}$$

$$Y_i = (r_0 + r(\theta))\sin(-\theta - (i-1)\beta), i = 1, 2 \ldots n \tag{20}$$

$$Z_i = r_0 \tan\alpha\theta, i = 1, 2 \ldots n \tag{21}$$

where p is the distance between the crossover points, a is the minor diameter of the yarn cross-section, r_0 is the radius of the tubular braid, $r(\theta)$ is the crimp of braiding yarn as a sine wave, β is the shift angle between the braiding yarns moving in the same direction, α is the braiding angle with the horizontal axes, n is the number of the braiding yarns revolving in the same direction, i is the counter defining the actual braiding yarn revolving in the same direction and θ is the wrapping angle (variable) around the mandrel ($0<\theta<2\pi$).

Equations for regular braid structure

The equations derived for the diamond braid can be used here but in the regular braid, each braiding yarn moving in the same direction crosses over two of the other set of yarns moving in the opposite direction so that the crossover points, as in the case of the 2/2 twill woven structures, but with a braiding angle to the horizontal axes are obtained. So some modifications are needed only with the equations derived to define the yarn path with the undulations and crossovers in the X^tY^t axes.

The braiding yarn moving in the counter-clockwise direction within regular braid structure is given in Figure 6 with X^1 to be the axes of the mentioned sine wave of the braiding yarn and Y^t axes which is perpendicular to ZX plane and X^t axes.

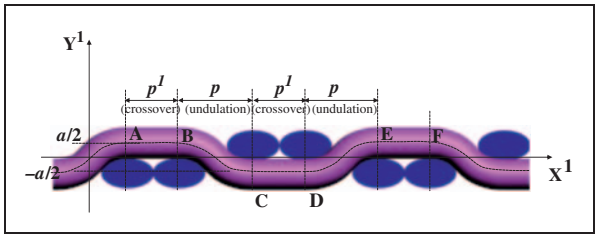

Figure 6. Crimp path of the braiding yarn revolving in the counter-clockwise direction for regular braid structure.

On the yarn path, it is assumed that for the crossover region (p^l) between the points A and B (Figure 6) the path is straight whereas for the undulation region (p) between the points B and C (Figure 6) the path is a sine wave. The period of the braiding yarn crimp is $2(p+p^l)$.

As there are straight parts and sinusoidal parts in the yarn path of the braiding yarn, the path shall be given as a discrete function of the wrapping angle θ and thus it is necessary to relate the period of yarn crimp and helical wrapping angle θ.

For this purpose, the undulation region of regular braid and diamond braid are assumed to be identical; so as the braiding yarn is wrapped helically around the mandrel with an angle of $\beta/2$, where β is the amount of wrapping to give the crimp ($2p$) of the diamond braid and has already been defined for the diamond braid, the braiding yarn will complete p as the undulation region in the regular braid structure.

There exists many studies on the calculations of the undulation (p) and crossover (p^l) regions, but as a common point p and p^l can be written in terms of the yarn's radius and thus in terms of each other. So a coefficient between p and p^l can be defined and used here as $p^l = pk_1$.

Now, a relationship can be obtained between the wrapping angle and the period of the crimp. To complete an undulation region of p, the braiding yarn is wrapped helically with an angle of $\theta = \beta/2$, in order to complete the crossover region of p^l the braiding yarn shall wrap by plus an angle of $k_1\beta/2$.

So the yarn crimp of the braiding yarns moving in the counter-clockwise direction can be written, as below, in terms of the wrapping angle (in Figure 6 from point A to E):

$$r(\theta) = \begin{cases} a/2 & ; 0 < \theta < k_1\beta/2 \\ a/2\sin\left(\frac{2\pi}{\beta}\theta + \frac{\pi}{2}\right) & ; k_1\beta/2 < \theta < (k_1+1)\beta/2 \\ -a/2 & ; (k_1+1)\beta/2 < \theta < (2k_1+1)\beta/2 \\ a/2\sin\left(\frac{2\pi}{\beta}\theta + \frac{\pi}{2}\right) & ; (2k_1+1)\beta/2 < \theta < (k_1+1)\beta. \end{cases} \quad (22)$$

The general yarn path of the yarns revolving in the counter-clockwise direction can be written considering the shift angle and the braiding yarn crimp as below;

$$r_0 = \frac{2(p+p^1)\cos\alpha}{\beta} \quad (23)$$

$$X_i = (r_0 + r(\theta))\cos(\theta + (i-1)\beta), i = 1, 2 \ldots n \quad (24)$$

$$Y_i = (r_0 + r(\theta))\sin(\theta + (i-1)\beta), i = 1, 2 \ldots n \quad (25)$$

$$Z_i = r_0 \tan\alpha\theta, i = 1, 2 \ldots n \quad (26)$$

And for the clockwise braiding yarns the yarn path can be given by the below equations:

$$r(\theta) = \begin{cases} -a/2 & ; 0 < \theta < k_1\beta/2 \\ a/2\sin\left(\frac{2\pi}{\beta}\theta + \frac{3\pi}{2}\right) & ; k_1\beta/2 < \theta < (k_1+1)\beta/2 \\ a/2 & ; (k_1+1)\beta/2 < \theta < (2k_1+1)\beta/2 \\ a/2\sin\left(\frac{2\pi}{\beta}\theta + \frac{3\pi}{2}\right) & ; (2k_1+1)\beta/2 < \theta < (k_1+1)\beta \end{cases} \quad (27)$$

$$r_0 = \frac{2(p+p^1)\cos\alpha}{\beta} \quad (28)$$

$$X_i = (r_0 + r(\theta))\cos(-\theta - (i-1)\beta), i = 1, 2 \ldots n \quad (29)$$

$$Y_i = (r_0 + r(\theta))\sin(-\theta - (i-1)\beta), i = 1, 2..n \quad (30)$$

$$Z_i = r_0 \tan\alpha\theta, i = 1, 2 \ldots n \quad (31)$$

where p is the length of the crossover region in the crimp path, p^l is the length of the undulation region in the crimp path, a is the minor diameter of the yarn cross-section, k_1 is the coefficient between p and p^l, r_0 is the radius of the tubular braid, $r(\theta)$ is the crimp of braiding yarn as a sine wave, β is the shift angle between the braiding yarns moving in the same direction, α is the braiding angle with the horizontal axes, n is the number of the braiding yarns revolving in the same direction, i is the counter defining the actual braiding yarn revolving in the same direction and θ is the wrapping angle (variable) around the mandrel ($0 < \theta < 2\pi$).

Equations for triaxial braid structure

The model creation for a triaxial diamond braid is given here. The axial yarns placed in the longitudinal direction of the structure are assumed to affect the crossover points by shifting the braiding yarns moving in the opposite direction and around the axial yarn with an amount equal to half of the minor diameter (a) of the axial yarn.

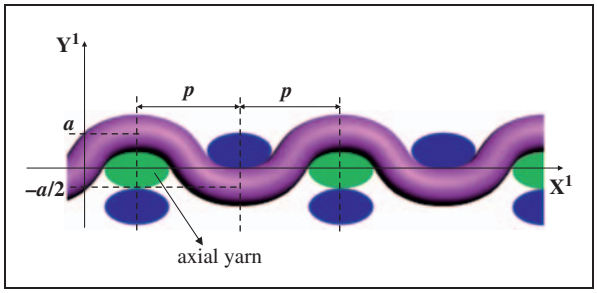

Figure 7. Crimp path of the braiding yarn revolving in the counter-clockwise direction for triaxial diamond braid structure.

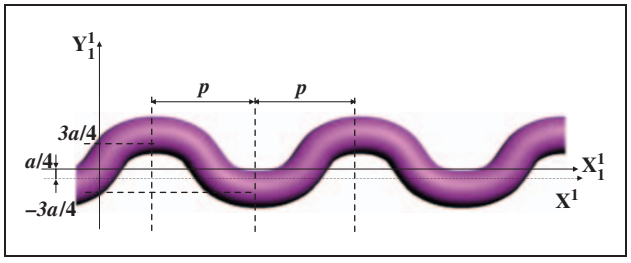

Figure 8. The braiding yarn of the triaxial structure moving in the counter-clockwise direction given as a sinusoidal wave.

When the axial yarns are placed at every crossover point in a diamond braid structure the difference in the equations when compared to an ordinary diamond braid will only be the change in the amplitude of the yarn crimp. So by only changing the crimp path as given below, the same equation set of the diamond braid (equations 13–15 and 19–21) can be used to obtain the yarn paths of such a triaxial diamond braid.

$$r(\theta) = a\sin\left(\frac{2\pi}{\beta}\theta + \frac{\pi}{2}\right) \text{ (for the braiding yarns moving in the counter} - \text{clockwise direction)} \tag{32}$$

$$r(\theta) = a\sin\left(\frac{2\pi}{\beta}\theta + \frac{3\pi}{2}\right) \text{ (for the braiding yarns moving in the clockwise direction)} \tag{33}$$

When the axial yarns are inserted at every two crossover points the axial yarn will shift the braiding yarns at these crossover points only (Figure 7).

In order to define the crimp path of such shifted braiding yarns using a sine wave, the amplitude of the yarn crimp is as $a_1 = 3a/2$ and such a braiding yarn moving in the counter-clockwise direction is given as a sinusoidal wave on $X'_1Y'_1$ axes in Figure 8. The same calculation methods are used as given for the diamond braid for the crimp period ($2p$), shift angle (β) and tubular braid radius (r_0).

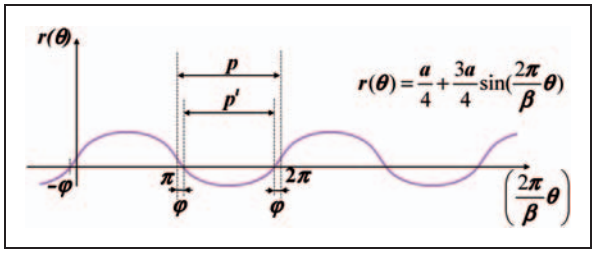

Figure 9. The distances between the crossover points of the braiding yarn moving in the counter-clockwise direction of the triaxial structure.

So the crimp path can be given in terms of helically wrapping angle θ on the axes system of $X'_1Y'_1$ as:

$$r_s(\theta) = \frac{3a}{4}\sin\left(\frac{2\pi}{\beta}\theta\right) \tag{34}$$

When this path is written according to the $X'Y'$ axes system the crimp path of the braiding yarn revolving in the counter-clockwise direction will be as:

$$r(\theta) = \frac{a}{4} + \frac{3a}{4}\sin\left(\frac{2\pi}{\beta}\theta\right) \tag{35}$$

However with this crimp path the distance for the crossover points gets narrower ($p'' < p$ in Figure 9) and thus the braiding yarn revolving in the opposite direction can not fit.

A coefficient is needed between p'' and p which will affect the radius of the tubular braid so that such a crimp path of sine wave can be used to give the yarn path of the braiding yarn in a triaxial diamond braid while the other set of yarns moving in the opposite direction can cross over/under.

Such a coefficient (k_2) can be obtained by proportioning the wrapping angles needed to obtain the distance, p' and p:

$$\frac{p}{p''} = \frac{\pi}{[(2\pi - \varphi) - (\pi + \varphi)]} \tag{36}$$

and

$$k_2 = \frac{p}{p''} \tag{37}$$

From here $k_2 = \frac{\pi}{\pi - 2\varphi}$ can be obtained where φ is the angle causing the difference in the distances between the crossover points. In order to find this angle φ, it is necessary to find the points at which the equation 35 crosses the X' axes (Figure 9).

Figure 10. Application of the model for diamond braid over the mandrel (a) front view, (b) top view of the drawings for the yarn paths (demonstrating yarn centrelines).

$$\frac{a}{4}+\frac{3a}{4}\sin\left(\frac{2\pi}{\beta}\theta\right)=0 \tag{38}$$

and from here $\varphi=\frac{2\pi}{\beta}\theta_1=19.5^\circ$ can be found and the coefficient (k_2) can be calculated.

Thus the general equations of triaxial (at every two crossovers) diamond braid for the braiding yarn in the counter-clockwise direction can be written as below:

$$r_0=k_2\frac{2p\cos\alpha}{\beta} \tag{39}$$

$$r(\theta)=\frac{a}{4}+\frac{3a}{4}\sin\left(\frac{2\pi}{\beta}\theta+\frac{\pi}{2}\right) \tag{40}$$

$$X_i=(r_0+r(\theta))\cos(\theta+(i-1)\beta), i=1,2\ldots n \tag{41}$$

$$Y_i=(r_0+r(\theta))\sin(\theta+(i-1)\beta), i=1,2\ldots n \tag{42}$$

$$Z_i=r_0(\tan\alpha)\theta, i=1,2\ldots n \tag{43}$$

Figure 11. Front view of diamond braid structure with multi-filament yarns drawn and rendered according to the present model by 3DS Max Studio.

and for the braiding yarn moving in the clockwise direction can be written as:

$$r_0=k_2\frac{2p\cos\alpha}{\beta} \tag{44}$$

$$r(\theta)=-\frac{a}{4}+\frac{3a}{4}\sin\left(\frac{2\pi}{\beta}\theta+\frac{3\pi}{2}\right) \tag{45}$$

$$X_i=(r_0+r(\theta))\cos(-\theta-(i-1)\beta), i=1,2\ldots n \tag{46}$$

$$Y_i=(r_0+r(\theta))\sin(-\theta-(i-1)\beta), i=1,2\ldots n \tag{47}$$

$$Z_i=r_0(\tan\alpha)\theta, i=1,2\ldots n \tag{48}$$

where p is the distance between the crossover points, a is the minor diameter of the yarn cross-section, r_0 is the radius of the tubular braid, $r(\theta)$ is the crimp of braiding yarn as a sine wave, β is the shift angle between the braiding yarns moving in the same direction, α is the braiding angle with the horizontal axes, n is the number of the braiding yarns revolving in the same

Figure 12. Application of the model for regular braid over the mandrel (a) front view, (b) top view of the drawings for the yarn paths (demonstrating yarn centrelines).

direction, i is the counter defining the actual braiding yarn revolving in the same direction and θ is the wrapping angle (variable) around the mandrel ($0<\theta<2\pi$).

Application of the model

The equations giving the yarn path of the braiding yarns for diamond, regular and triaxial diamond braid are derived and with the aid of visual basic programming the coordinates of the points giving the 3D path of the braiding yarns are obtained.

The paths of the yarns are drawn three-dimensionally with the aid of 3DSMax Studio and in order to draw the structures with each program, braid angle (α), flattening coefficient of the yarns (e), and number of the braiding yarns moving in the same direction (n), are given as input data: $\alpha = 45^\circ$, $e = 0.5$, $n = 8$ and for the regular braid $k_1 = 1$ is considered.

In order to maintain a realistic look, the yarns are drawn to be multifilament yarns with exact cross-sections by filling the elliptical cross-section of the braiding and axial yarns with filament fibres of circular cross-sections and rendered views are obtained with the aid of 3DSMax Studio.

Figure 13. Front view of regular braid structure with multifilament yarns drawn and rendered according to the present model by 3DS Max Studio.

3D yarn paths of the diamond tubular braid with a total of 16 yarns are given in Figure 10a and 10b, as front and top views, by demonstrating the yarn centrelines and the centrelines of the yarns braiding in the same direction are given in the same colour. The rendered view of the diamond tubular braid using multifilament yarns is given in Figure 11. For regular tubular braid with a total of 16 yarns, 3D yarn paths are given in Figure 12a and 12b, as front and top views, and the rendered view of the regular tubular braid by using multifilament yarns is given in Figure 13. 3D yarn paths and the rendered views of the triaxial tubular braid with 16 yarns braiding and eight straight yarns are given in Figures 14 and 15. Side views for the 3D paths are not given for any of the structures because as the braids are tubular, side and front views will be the same. In the top views of the 3D yarn paths for all of the structures, the crimp as a path with sine wave can clearly be seen. Also, it is possible to observe the placement of straight yarns at the crossovers in Figure 14b.

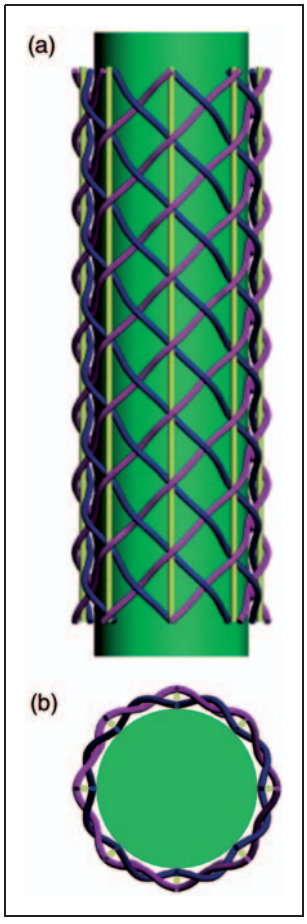

Figure 14. Application of the model for triaxial braid over the mandrel (a) front view, (b) top view of the drawings for the yarn paths.

Figure 15. Front view of triaxial braid structure with multifilament yarns drawn and rendered according to the present model by 3DS Max Studio (demonstrating yarn centrelines).

Discussion

For the simplicity of the model, the cross-sections of the yarns are assumed to be elliptical within the braided structures by inputing a value for the flattening coefficient. However, it is possible to include any yarn cross-section based on Kemp's or Hamilton's assumptions within the equations and programs.

The distances between the crossover points of the braiding yarns are assumed to be $p = 2.5b$, where b is the major diameter of the yarn cross-section, because the yarns were assumed to have elliptical cross-sections and slack structures were considered. However, if the yarns are considered to have cross-sections other than elliptical, the appropriate equation giving the distances between the crossover points along the braiding yarn will be included in the calculations of the model and the programs.

After all, it is possible to use the general equations given to obtain the yarn paths by considering the yarn undulation with different yarn cross-sections and, thus, different distances between the crossover points along the braiding yarn equations are used. In addition, the model is versatile enough to be adapted for the mandrels with variable cross-sections.

With a tight structure, the cross-section of the braiding yarns will be flattened in addition to being compressed, also shifting of the braiding yarns will occur on the Z axis of the ZX plane of the braiding yarn while helically wound onto the mandrel. So in case of a tight structure, these facts shall also be considered by defining the $Z(\theta)$ as a discrete function, however, tight structures are not preferable for load bearing applications due to the divergence in the axes of the braiding yarns in accordance with the load direction.

The application of the model was done considering 16 yarns with 0.5 as the flattening coefficient and a 45° braid angle for all of the structures, however any number of yarns with any flattening coefficient can be braided by inputting any number as 'n' with any value for the braid angle. For the application, 3DSMax Studio was preferred because it is a 3D modelling, animation, and rendering program which features realistic appearances and it was used only to express the yarn paths in 3D after obtaining the yarn paths from the equations by entering practical data as input. Any

such software other than 3DSMax can also be utilized to observe the obtained yarn paths in 3D.

Conclusion

A geometrical model, which is simple and versatile, is proposed to simulate three-dimensional yarn paths of the braided structures and the proposed model is applicable for different braid structures and also braids with different structural parameters such as braid angle, number of braiding yarns (horn gears), etc.

3D yarn paths for diamond, regular and triaxial diamond braid have been geometrically obtained via the proposed model. Slack structures of them have been simulated by drawing and rendering in 3D with the aid of Visual Basic and 3DSMax Studio programs. The application of the model for tighter tubular braids and for braiding on mandrels with variable cross-sections has been left for future work.

With the proposed model the braided structures can be simulated so that the structures can be modified for desired performance criteria prior to manufacture and it is also possible to visualize braided structures under different loadings as different braid angles can be input into the proposed model. By including the appropriate equations within the program the yarn consumptions can be calculated.

Funding

This research received no specific grant from any funding agency in the public, commercial, or not-for-profit sectors.

References

1. Brunnschweiler B. The structure and tensile properties of braids. *J Textile Inst* 1954; 45: T55–T87.
2. Zhang Q, Beale D, Adanur S, Brouhgton RM and Walker RP. Structural analysis of two-dimensional braided fabrics. *J Textile Inst* 1997; 88: 41–52.
3. Phoenix SL. Mechanical response of a tubular braided cable with an elastic core. *Textile Res J* 1978; 48: 81–91.
4. Wu H, Seo M, Becker S and Mandel JF. Structural modeling of double-braided synthetic fibre ropes. *Textile Res J* 1995; 65: 619–631.
5. Hristrov K, Armstrong-Carroll E, Dunn M, Pastore C and Gowayed Y. Mechanical behavior of circular hybrid braids under tensile loads. *Textile Res J* 2004; 74: 20–26.
6. Carey J, Munro M and Fahim A. Longitudinal elastic modulus prediction of a 2-D braided fibre composite. *J Reinf Plast Compos* 2003; 22: 813–831.
7. Hopper R, Grant W and Popper P. Mechanics of hybrid braid with an elastic core. *Textile Res J* 1998; 65: 709–722.
8. Yüksekkaya M and Adanur S. Analysis of polymeric braided tubular structures intended for medical applications. *Textile Res J* 2009; 79: 99–109.
9. Ayranci C and Carey J. 2D braided composites: a review for stiffness critical applications. *Compos Struct* 2008; 85: 43–58.
10. Endruweit A and Long AC. A model for the in-plane permeability of triaxially braided reinforcements. *Compos Part:A Appl Sci Manuf* 2011; 42: 165–172.
11. Byun JH. The analytical characterization of 2D braided textile composites. *Compos Sci Technol* 2000; 60: 705–716.
12. Ivanov D, Baudry F, Broucke BVD, Lomov S, Xie H and Verpoest I. Failure analysis of triaxial braided composite. *Compos Sci Technol* 2009; 69: 1372–1380.
13. Zhang P, Gui L and Fan Z. An analytical model for predicting the elastic properties of triaxially braided composites. *J Reinf Plast Compos* 2009; 28: 1903–1916.
14. Xiao X, Kai HG and Gong X. Strength predictions of a triaxially braided composite. *Compos Part:A Appl Sci Manuf* 2011; 42: 1000–1006.
15. Lomov SV, Parnas RS, Ghosh SB, Verpoest I and Nakai A. Experimental and theoretical characterization of the geometry of two-dimensional braided fabrics. *Textile Res J* 2002; 72: 706–712.
16. Liao T and Adanur S. 3D Structural simulation of tubular braided fabrics for net-shape composite. *Textile Res J* 2000; 70: 297–303.
17. Potluri P, Rawal A, Rivaldi M and Porat I. Geometrical modeling and control of a triaxial braiding machine for producing 3D performs. *Compos Part:A Appl Sci Manuf* 2003; 34: 481–492.
18. Rawal A, Potluri P and Steele C. Geometrical modelling of the yarn paths in three-dimensional braided structures. *J Indust Text* 2005; 35: 115–226.